Neutron diffraction and polarimetric study of the magnetic and crystal structures of $HoMnO_3$ and $YMnO_3$

2006 J. Phys.: Condens. Matter 18 10085

(http://iopscience.iop.org/0953-8984/18/44/008)

INSTITUTE OF PHYSICS PUBLISHING JOURNAL OF PHYSICS: CONDENSED MATTER

J. Phys.: Condens. Matter **18** (2006) 10085–10096 doi:10.1088/0953-8984/18/44/008

Neutron diffraction and polarimetric study of the magnetic and crystal structures of $HoMnO_3$ and $YMnO_3$

P J Brown[1,2] **and T Chatterji**[1]

[1] Institut Laue Langevin, BP 156, 38042 Grenoble, France
[2] Department of Physics, Loughborough University, Loughborough LE11 3TU, UK

Received 4 September 2006, in final form 4 October 2006
Published 20 October 2006
Online at stacks.iop.org/JPhysCM/18/10085

Abstract

We have undertaken a new study of the magnetic and crystalline structures of $YMnO_3$ and $HoMnO_3$ using neutron diffraction combined with neutron polarimetry. It is shown how the long-standing problem of distinguishing between magnetic structure models which give nearly identical diffraction intensities may be resolved. The experiments show that the magnetic structure of $YMnO_3$ has space group $P6'_3$ (or $P6_3$) rather than $P6'_3cm'$ (or $P6_3cm$) with Mn moments of 3.14(3) μ_B inclined at 11(1)° to [10.0] (or [12.0] for $P6_3$) in the (00.1) plane. For $HoMnO_3$ the experiments confirm the $P6'_3c'm$ symmetry at 50 K and the spin-rotation transition leading to a low-temperature structure with magnetic space group $P6'_3cm'$. In this structure both the Ho1 and Ho2 moments can order with spins parallel to [00.1] in ferromagnetic layers, antiferromagnetically coupled. The Ho1 and Ho2 moments in neighbouring layers are found to be oppositely oriented. The ordered moments at 2 K are 3.32(8), 4.17(13) and 1.31(11) μ_B on the Mn, Ho1 and Ho2 atoms respectively. No evidence was found, in this zero-field study, for the magnetic transition at ≈5 K reported in the literature (Lottermoser *et al* 2004 *Nature* **30** 541; Vajk *et al* 2005 *Phys. Rev. Lett.* **94** 87601). Nuclear structure refinements show that in $YMnO_3$ at 10 K and in $HoMnO_3$ at all temperatures below 50 K any deviation of the manganese x parameter from 1/3 is less than 0.0008.

1. Introduction

There has been a recent renewal of interest in the hexagonal manganates $RMnO_3$, R = Er, Ho, In, Lu, Tm, Sc, Y, (space group $P6_3cm$) as they belong to the rare class of multiferroic materials which exhibit both ferroelectricity and magnetic order. The ferroelectric transition temperature $T_C \approx 1000$ K and magnetic order develops in the Mn sub-lattices below $T_N \approx 100$ K [1]. When the R ion is also magnetic, the interactions between the different triangular anti-ferromagnetic sub-lattices generate complex magnetic phase diagrams. The

coexistence of ferroelectric and magnetic order offers the possibility of exploiting their mutual coupling and that of each of them to external fields in 'spintronic' devices. It has recently been shown that $HoMnO_3$ and the Tb and Dy members of the orthorhombic RMn_2O_3 series can develop magneto-electric polarizations which are orders of magnitude larger than those associated with normal magneto-electric crystals such as Cr_2O_3 [2]. Although $YMnO_3$ is not magneto-electric, it does have a dielectric anomaly associated with the Néel transition [3] and it has been shown that there is strong coupling between the ferroelectric and magnetic domain walls [4]. The hexagonal manganates are also interesting because of their low dimensionality and the geometrical frustration associated with the triangular arrangement of the manganese atoms [3]. Recent inelastic neutron scattering investigations [5, 6] on $YMnO_3$ gave evidence for coexistence of the anti-ferromagnetic Néel, and competing spin liquid, states of the frustrated triangular lattice. However, attempts to solve problems associated with the coupling of two order parameters or competition between the Néel and spin liquid states rely on a knowledge of the magnetic structures which have been uncertain because of near homometry between different possible magnetic configurations.

The magnetic ordering in both $YMnO_3$ and $HoMnO_3$ has already been intensively investigated using unpolarized neutron powder and single crystal diffraction [7–11] and second harmonic generation (SHG) [12]. However, due to difficulties associated with homometry between possible anti-ferromagnetic configurations of Mn [8] and the inability of SHG to distinguish the different magnetic sub-lattices, the magnetic structures of the different phases which occur is still controversial [9, 10]. For $HoMnO_3$, the SHG results suggest that at $T_N \approx 75$ K the Mn moments order to an anti-ferromagnetic arrangement with magnetic space group $P6'_3c'm$. On cooling below T_N there is evidence for two further magnetic phase transitions [10]. Between 45 and 35 K there is a first-order transition in which the Mn spins rotate by 90° as the magnetic symmetry changes to $P6'_3cm'$ [12], and at $T \approx 5$ K it is suggested that a second phase transition between nearly homometric magnetic structures with space groups $P6_3cm$ and $P6'_3cm'$ is triggered by Ho ordering. In $YMnO_3$ with only a single magnetic species, the phase diagram is much simpler and a single magnetically ordered phase is stable below the Néel temperature of 65 K.

Homometry between significantly different structures arises because in a conventional neutron scattering experiment only the reflection intensities are measured. The difference between homometric structures is manifest in the relative phases of their nuclear and magnetic structure factors and these can, in favourable cases, be measured using neutron polarimetry. This paper describes experiments in which spherical neutron polarimetry (SNP) has been used to study the magnetic structures of $YMnO_3$ and the different magnetic phases of $HoMnO_3$. Since the interpretation of the results depends critically on a knowledge of the nuclear structure factors we have also determined the crystal structure parameters of $YMnO_3$ at 10 K and those of $HoMnO_3$ as a function of temperature between 2 and 50 K.

2. Crystal and magnetic structures

Details of the crystal structure of the hexagonal rare-earth manganates are given in table 1. The non-centrosymmetric structure is built from six layers of O atoms equally spaced at intervals of 1/6 along the c-axis [12, 13]. There are Mn atoms in every third O layer and the rare-earth atoms lie between the O layers which contain no Mn. The Mn moments order anti-ferromagnetically at $T_N \approx 66$ K in $YMnO_3$ and at $T_N \approx 75$ K in $HoMnO_3$ [7, 14, 8]. The different possible magnetic structures of $YMnO_3$ are discussed in detail by Bacon [15]. The x coordinate of the Mn atoms is very close to 1/3 and this leads to near equality of the magnetic structure factors for pairs of possible structures with different magnetic space groups

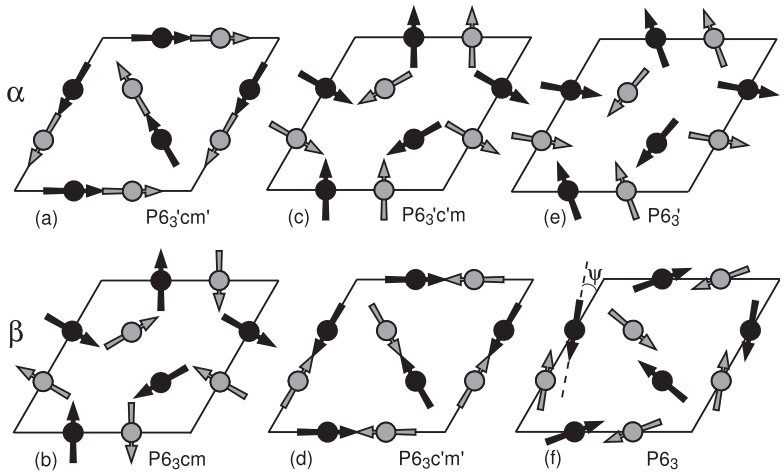

Figure 1. Different possible ordered arrangements of Mn spins in the hexagonal rare-earth manganates.

Table 1. Crystal structure data for hexagonal $RMnO_3$ compounds [13].

Space group $P6_3cm$			$a \approx 6.12, c \approx 11.4$ Å		
Atom	Position		x	y	z
Mn	6(c)	$x, 0, z$	≈1/3	0	0
R1	2(a)	$0, 0, z$	0	0	≈1/4
R2	4(b)	$1/3, 2/3, z$	1/3	2/3	≈1/4
O1	4(c)	$x, 0, z$	≈1/3	0	≈1/6
O2	4(c)	$x, 0, z$	≈1/3	0	≈1/3
O3	2(a)	$0, 0, z$	0	0	≈1/2
O4	4(b)	$1/3, 2/3, z$	1/3	2/3	≈0

(homometry). In each pair, one of the structures was denoted α and the other β. In the α structures the spins on manganese atoms at $-x, -y, \frac{1}{2}$ are parallel to those at $x, y, 0$, whereas in the β structures they point in opposite directions. The different possible configurations are indicated schematically in figures 1(a)–(f). Each homometric pair is characterized by the angle ψ between the spin direction of an Mn atom and the axis on which it lies. An α and a β structure are homometric when $\psi_\alpha = \psi_\beta \pm 90°$. In the magnetic space groups of the α structures the 6_3 axis is combined with time reversal, and in the β structures it is not. In the structures (e) and (f) of figure 1 the symmetry planes of $P6_3cm$ are not in the magnetic group and the angle ψ can adopt any value. The structures in which these planes are retained, constraining ψ to special values, are shown in figures 1(a)–(d). They are labelled with the magnetic space group to which they belong. The original single crystal study enabled the pair (c), (d) to be selected on the basis of the reflection intensities [8]. The homometry is exact only if the Mn positional parameter $x = 1/3$, but the reflection intensities from the two structures are still very nearly equal even if x differs from $1/3$ by as much as 0.02. However, it is significant that only the symmetries in which the six-fold axis is not combined with time reversal will allow a magneto-electric effect.

The difference between the two members of a homometric pair shows up in the phase relationships between the magnetic interaction vectors and the nuclear structure factors. This phase difference can be expressed as $\phi = \phi_N - \phi_M$, where $\phi_N = \tan^{-1} \mathrm{i}(N^* - N)/(N^* + N)$

is the phase of the complex nuclear structure factor N and ϕ_M is the phase of the magnetic interaction vector. The magnetic structure factors of the $h0.l$ reflections of $YMnO_3$ can be written in terms of their components M_{a*} parallel to $\mathbf{a}^*$ and M_b parallel to $\mathbf{b}$ as

$$M_{a*}(k) = \mu f(k)\left(\left[-(1-G)\sin\psi + \mathrm{i}\sqrt{3}G'\cos\psi\right] \pm \left[-(1-G)\sin\psi + \mathrm{i}\sqrt{3}G'\cos\psi\right]\right) \tag{1}$$

$$M_b(k) = \mu f(k)\left(\left[(1-G)\cos\psi + \mathrm{i}\sqrt{3}G'\sin\psi\right] \pm \left[(1-G)\cos\psi + \mathrm{i}\sqrt{3}G'\sin\psi\right]\right) \tag{2}$$

$$\text{where } G = \cos 2\pi h x_{\mathrm{Mn}} \quad \text{and} \quad G' = \sin 2\pi h x_{\mathrm{Mn}}$$

μ is the manganese moment and $f(k)$ its form factor. For the α structures the plus sign applies to the even l reflections and the minus sign to the odd l ones. For the β structures the reverse is true. If $x_{\mathrm{Mn}} = 1/3$, $G = -1/2$ and $G' = \pm\sqrt{3}/2$ so that $|1-G| = |\sqrt{3}G'| = 3/2$. When the $h0.l$ reflections are in the scattering plane the components of the magnetic interaction vector $\mathbf{M}_\perp(\mathbf{k}) = \hat{\mathbf{k}} \times \mathbf{M}(k) \times \hat{\mathbf{k}}$, parallel ($M_{\perp y}$) and perpendicular ($M_{\perp z}$) to the scattering plane are

$$M_{\perp y}(k) = M_{a*}(k)\cos\alpha \qquad \text{and} \qquad M_{\perp z}(k) = M_b(k) \tag{3}$$

with $\alpha = \tan^{-1} ha^*/lc^*$.

3. Neutron polarimetry

In a neutron scattering experiment the relationship between the polarizations of the incident and scattered beams $\mathbf{P}$ and $\mathbf{P}'$ can be conveniently expressed by the tensor equation [16]

$$\mathbf{P}' = \mathcal{P}\mathbf{P} + \mathbf{P}'' \tag{4}$$

where $\mathcal{P}$ is a tensor which describes the rotation of the polarization and $\mathbf{P}''$ is the polarization created in the scattering process. The polarization directions are defined here with respect to right-handed orthogonal polarization axes with x parallel to the current scattering vector $\mathbf{k}$ and z perpendicular to the scattering plane ([01.0] for $h0.l$ reflections). With this definition there is no component of the magnetic interaction vector parallel to x.

$$\mathcal{P} = \begin{pmatrix} (N^2 - M^2)/I_0 & 2NM_{\perp z}x\sin\phi/I_0 & 2N(M_{\perp y})\sin\phi/I_0 \\ -2NM_{\perp z}\sin\phi/I_y & (I_0 - 2|M_{\perp z}|^2)/I_y & 2M_{\perp y}M_{\perp z}/I_y \\ -2NM_{\perp y}\sin\phi/I_z & 2M_{\perp y}M_{\perp z}/I_z & (I_0 - 2|M_{\perp y}|^2)/I_z) \end{pmatrix} \tag{5}$$

$$\mathbf{P}'' = \begin{pmatrix} 0 \\ 2NM_{\perp y}\cos\phi/I \\ 2NM_{\perp z}\cos\phi/I \end{pmatrix} \qquad \begin{aligned} M^2 &= |M_{\perp y}|^2 + |M_{\perp z}|^2 \\ I_0 &= M^2 + |N|^2 \\ I_y &= I_0 + 2P_y NM_{\perp y}\cos\phi \\ I_z &= I_0 + 2P_z NM_{\perp z}\cos\phi \\ I &= I_y + I_z - I_0. \end{aligned} \tag{6}$$

The components $M_{\perp y}$ and $M_{\perp z}$ for the $h0.l$ reflections for the different models are those given in table 2.

The quantities which are measured in a polarimetric experiment are the components of the polarization matrix P. The component P_{ij} of P is the polarization parallel to i of the scattered beam when the incident polarization is parallel to j.

$$\mathsf{P}_{ij} = \left\langle \mathcal{P}_{ij} + \mathrm{P''}_i \right\rangle \tag{7}$$

where the angle brackets indicate an average over all the different magnetic domains and nuclear twins which contribute to the reflection.

Table 2. Relative magnitudes and phases of the magnetic interaction vectors, of $h0.l$ reflections, for different magnetic structural models of $YMnO_3$. The components are given with respect to the polarization axes.

Model	Sp. group	Parity	$M_{\perp y}$ [a]	$M_{\perp z}$ [a]	ϕ_M
α series	$P6'_3cm'$	l odd	$i\sqrt{3}G'\cos\alpha$	0	$\frac{\pi}{2}$
		l even	0	$1-G$	0
	$P6'_3c'm$	l odd	0	$i\sqrt{3}G'$	$\frac{\pi}{2}$
		l even	$-(1-G)\cos\alpha$	0	π
	$P6'_3$	l odd	$i\sqrt{3}G'\cos\psi\cos\alpha$	$i\sqrt{3}G'\sin\psi$	$\frac{\pi}{2}$
		l even	$-(1-G)\sin\psi\cos\alpha$	$(1-G)\cos\psi$	$\pi, 0$
β series	$P6_3cm$	l odd	$-(1-G)\cos\alpha$	0	π
		l even	0	$i\sqrt{3}G'$	$\frac{\pi}{2}$
	$P6_3c'm'$	l odd	0	$1-G$	0
		l even	$i\sqrt{3}G'\cos\alpha$	0	$\frac{\pi}{2}$
	$P6_3$	l odd	$-(1-G)\sin\psi\cos\alpha$	$(1-G)\cos\psi$	$\pi, 0$
		l even	$i\sqrt{3}G'\cos\psi\cos\alpha$	$i\sqrt{3}G'\sin\psi$	$\frac{\pi}{2}$

[a] The values given are divided by $\mu f(k)$.

Table 3. Diagonal elements of the polarization matrices measured for $h0.l$ reflections from $YMnO_3$ at 4 K.

l even				l odd			
hkl	P_{xx} [a]	P_{yy} [a]	P_{zz} [a]	hkl	P_{xx} [a]	P_{yy} [a]	P_{zz} [a]
100	−0.889(1)	−0.894(1)	0.98(2)	101	−0.90(1)	0.67(2)	−0.59(1)
102	−0.717(6)	−0.694(3)	0.96(1)	103	−0.942(7)	0.88(2)	−0.84(1)
104	−0.859(7)	−0.79(2)	0.90(4)	105	−0.94(3)	0.93(1)	−0.83(5)
200	−0.74(4)	−0.909(4)	0.82(5)				
202	0.426(4)	0.420(3)	0.99(1)				
204	0.056(2)	0.068(3)	0.99(1)				

[a] $x \parallel hk.l$, $y \perp hk.l$ and [01.0], $z \parallel$ [01.0].

4. Experimental details

4.1. Polarized neutron scattering

The work was carried out on the high flux reactor of the Institut Laue Langevin, Grenoble. The crystals of $YMnO_3$ and $HoMnO_3$ were grown by flux melting with a $PbO–PbF_2$ flux and were kindly given to us by Dr K Kohn. For the measurements on $YMnO_3$ the zero-field polarimeter CRYOPAD II [17] was installed on the polarized triple-axis spectrometer IN20. The crystal, mounted in a standard orange cryostat, was placed at the centre of the cylindrical zero-field region and maintained at a temperature of 4 K throughout the experiment. The crystal was aligned with [01.0] vertical so that $h0.l$ reflections were in the scattering plane. All 9 components of the polarization matrices were measured for 19 $h0.l$ reflections at a wavelength of 2.36 Å and for 17 reflections at the shorter wavelength 1.53 Å. No significant off-diagonal components were observed, nor was any polarization dependence of the scattered intensity detected. Equivalent measurements made on the same reflections at the two wavelengths were in good agreement. A synthesis of the results obtained, averaged over equivalent reflections and over the two wavelengths, is given in table 3.

The experiments on $HoMnO_3$ were made with CRYOPAD II installed on the hot source polarized neutron diffractometer D3; the polarization of the scattered beam was measured using a spin polarized ^{3}He filter placed inside a constant field enclosure [18]. Initially the crystal was

Table 4. Diagonal elements of the polarization matrices of $h0.l$ reflections of $HoMnO_3$ measured at 50, 20 and 2 K.

	l even				l odd			
T (K)	hkl	P_{xx}	P_{yy}	P_{zz}	hkl	P_{xx}	P_{yy}	P_{zz}
	100	0.4(2)	2(2)	0.3(2)	101	−1.003(13)	−0.972(10)	1.023(11)
	102	−0.254(13)	1.00(2)	−0.242(12)	103	−0.92(2)	−0.89(2)	1.00(2)
50	104	−0.82(2)	0.94(3)	−0.82(3)	105	−0.81(8)	−0.86(8)	0.91(7)
	200	−0.2(1.0)	0.8(5)	0.7(4)				
	202	0.89(2)	1.00(2)	0.90(2)				
	204	0.63(6)	0.97(6)	0.49(5)				
	100	−1.038(12)	−0.99(2)	1.03(7)	101	−0.29(10)	0.71(12)	−0.13(11)
	102	−0.681(10)	−0.67(2)	1.02(2)	103	−0.98(2)	0.99(2)	−0.96(2)
20	104	−0.92(2)	−0.90(2)	0.99(3)	105	−0.85(9)	0.90(10)	−0.75(8)
	200	−0.86(2)	−0.82(3)	0.98(3)				
	204	0.17(3)	0.19(3)	0.99(4)				
	100	−0.966(8)	−0.94(2)	0.966(12)	101	−0.92(2)	0.974(14)	−0.91(2)
	102	−0.674(7)	−0.686(7)	1.00(3)	103	−0.984(4)	0.996(4)	−0.996(11)
2	104	−0.90(2)	−0.90(2)	0.97(2)	105	−1.02(13)	0.94(9)	−0.74(11)
	200	−0.86(2)	−0.87(2)	1.00(2)				
	202	0.418(14)	0.408(11)	0.988(11)				
	204	0.14(3)	0.20(2)	0.98(3)				

mounted with [01.0] vertical and measurements of the polarization matrices of a set of $h0.l$ reflections made at temperatures of 50, 20 and 1.8 K. The crystal was remounted with $[\bar{1}1.0]$ vertical and the polarization matrices of some $hh.l$ reflections measured at 1.8 K. Again no significant off-diagonal components were found. The averaged results for the diagonal terms are summarized in tables 4 and 7.

4.2. Integrated intensity measurements

It can be seen from equation (6) that a good knowledge of the nuclear structure factors N is needed to interpret the polarimetric measurements. For this reason unpolarized neutron diffraction measurements have been made on both the $YMnO_3$ and $HoMnO_3$ crystals to determine their structural parameters. The measurement were made on the hot-source four-circle diffractometer D9, using a neutron wavelength $\lambda = 0.84$ Å. The crystals were cooled by a two-stage Displex refrigerator fitted with a Joule–Thomson third stage. The integrated intensities of a set of 1417 reflections with $\sin\theta/\lambda < 0.95$ Å^{-1} were measured from $YMnO_3$ at 10 K. For $HoMnO_3$ it has been reported that the x parameter of Mn changes significantly in the temperature range 2–40 K [2]; so a set of 750 reflections with $\sin\theta/\lambda < 0.92$ Å^{-1} were measured at 50, 20 and 2 K, and a restricted set containing 250 of the low angle reflections at temperatures of 4, 6, 8, 10 and 15 K. The measured intensities were corrected for absorption and averaged over equivalents, yielding 590 independent reflections for $YMnO_3$. For $HoMnO_3$ there were 309 and 68 reflections in the full and low-angle sets respectively.

5. Analysis of the results

5.1. Crystal structure analysis

The structure factors derived from the integrated intensity measurements were used in least squares refinements to determine the positional and thermal parameters. A single extinction

Table 5. Crystal structure parameters determined for $YMnO_3$ at 10 K and for $HoMnO_3$ at 50, 20 and 2 K.

Parameter		$YMnO_3$	$HoMnO_3$		
		10 K	50 K	20 K	2 K
Mn	x	0.3335(6)	0.3337(5)	0.3340(8)	0.3340(5)
	B[a]	0.41(2)	0.56(4)	0.53(5)	0.46(5)
	μ (μ_B)	3.35(6)	2.67(5)	3.17(7)	3.32(8)
R1[b]	z	0.2735(4)	0.2794(9)	0.2804(11)	0.2791(11)
	B[a]	0.21(2)	0.03(3)	0.05(4)	0.03(4)
	μ (μ_B)		0.27(8)	−1.30(11)	−4.17(13)
R2[b]	z	0.2312(4)	0.2353(8)	0.2362(8)	0.2355(10)
	B[a]	0.22(2)	0.14(3)	0.12(3)	0.13(4)
	μ (μ_B)			−0.04(9)	1.31(11)
O1	x	0.3070(3)	0.3071(3)	0.3067(4)	0.3061(4)
	z	0.1621(4)	0.1654(9)	0.1668(11)	0.1655(12)
	B[a]	0.35(2)	0.36(3)	0.34(3)	0.36(3)
O2	x	0.6409(3)	0.6404(3)	0.6401(5)	0.6397(5)
	z	0.3356(4)	0.3381(9)	0.3395(10)	0.3386(11)
	B[a]	0.37(2)	0.42(3)	0.41(3)	0.36(3)
O3	z	0.4762(5)	0.4813(10)	0.4817(12)	0.4813(13)
	B[a]	0.35(3)	0.49(6)	0.45(7)	0.50(7)
O4	z	0.0181(4)	0.0232(8)	0.0240(9)	0.0236(11)
	B[a]	0.40(2)	0.33(4)	0.36(5)	0.35(5)
Extinction		0.027(3)	0.128(9)	0.122(9)	0.134(12)
R_{cryst}		5.2	5.0	4.9	5.3

[a] Isotropic temperature factor ($Å^2$).
[b] R = Y or Ho.

parameter, the mosaic spread of the Becker–Coppens type 1 model [19], was included in the refinement. The results obtained from the full data sets are shown in table 5. The values given for the moments are those obtained using the magnetic models derived in the following sections from the polarized neutron data.

5.2. Magnetic structure of $YMnO_3$

Some qualitative conclusions can be drawn immediately from the observations given in table 3. The $h0.l$ reflections with odd l have zero nuclear structure factors due to the systematic absence imposed by the c glide plane of $P6_3cm$. For these reflections P_{xx} and P_{zz} are negative whilst P_{yy} is positive. The major component of $\mathbf{M}_\perp$ for these reflections is therefore parallel to y. However, the absolute values of both P_{yy} and P_{zz} are significantly less than 1. This depolarization effect is most marked in the {10.1} reflections where $\mathsf{P}_{yy} \approx -\mathsf{P}_{zz} \approx 0.6$. It shows that the magnetic interaction vector of the odd-l reflections must have a non-zero z component and the crystal contain equal numbers of domains in which the direction of this component is reversed. Referring to table 2, it can be seen that this observation is only compatible with the $P6_3$ and $P6_3'$ structures in which the moment can assume a general direction in the (00.1) plane. The two domains with opposite $M_{\perp z}$ components are related by the mirror planes which no longer belong to the magnetic symmetry group.

For a quantitative analysis of the results all the different types of domain expected to be present must be taken into account. Since the structure is ferroelectric, twins with opposite

Table 6. Values of the phase factors $\cos\phi$ and $\sin\phi$ for different combinations of ferroelectric and magnetic 180° domains.

		α series			β series		
FE	AF	ϕ	$\cos\phi$	$\sin\phi$	ϕ	$\cos\phi$	$\sin\phi$
+	+	ϕ_N	$\cos\phi_N$	$\sin\phi_N$	$\phi_N + \frac{\pi}{2}$	$-\sin\phi_N$	$\cos\phi_N$
+	−	$\phi_N + \pi$	$-\cos\phi_N$	$\sin\phi_N$	$\phi_N - \frac{\pi}{2}$	$\sin\phi_N$	$-\cos\phi_N$
−	+	$-\phi_N$	$\cos\phi_N$	$-\sin\phi_N$	$-\phi_N + \frac{\pi}{2}$	$-\sin\phi_N$	$\cos\phi_N$
−	−	$-\phi_N + \pi$	$-\cos\phi_N$	$-\sin\phi_N$	$-\phi_N - \frac{\pi}{2}$	$\sin\phi_N$	$-\cos\phi_N$

Table 7. Diagonal elements of the polarization matrices of $hh.l$ reflections of $HoMnO_3$ measured at 1.8 K.

	l odd					l even			
hhl	P_{xx}	P_{yy}	P_{zz}	I^a	hhl	P_{xx}	P_{yy}	P_{zz}	I^a
111	0.85(2)	0.99(2)	0.85(2)	1	112	0.80(1)	0.81(1)	0.82(1)	2
113	0.78(2)	0.79(2)	0.78(2)	61					
115	0.23(9)	0.67(8)	0.27(9)	0.2					
117	0.86(8)	0.87(6)	0.83(3)	3					
223	0.77(1)	0.75(1)	0.79(1)	53	222	0.85(6)	0.74(6)	0.71(6)	2
225	0.3(2)	0.7(2)	0.1(2)	0.1	226	1.01(2)	0.97(2)	0.99(2)	10
227	0.68(5)	0.82(6)	0.61(5)	3					

[a] Observed peak count per s.

ferroelectric polarities can occur. We attempted to favour a single twin polarity by applying electric field while quenching the $YMnO_3$ crystal from the para-electric into the ferroelectric phase. There can also be 180° magnetic domains corresponding to regions of crystal in which all the magnetic moments are reversed. The ferroelectric twins have equal and opposite values of the phase offset ϕ_N, and ϕ_M for the two 180° domains differs by π. The combined phase offset affects the scattered polarization of the even-l reflections for which $N \neq 0$ and for these reflections ϕ_M is 0 or π for the α series and $\pm\pi/2$ for the β series. Four different combinations of the domains are possible giving the different values of ϕ indicated in table 6. If the average value of $\cos\phi$ is non-zero then the scattered intensity is polarization dependent since one or both of I_y and I_z (equation (6)) will differ from I_0. No such variation was observed in the experiment, indicating that the domains with opposite values of $\cos\phi$ are equally populated. A non-zero average for $\sin\phi$ would give non-zero values for one or both of the pairs of components P_{xz}, P_{zx} and P_{xy}, P_{yx}. Again none of these components was significantly different from zero, showing that in spite of the field treatment all four combinations of domains were equally present. In the absence of an imbalance in the 180° domains, distinction between the α and β configurations cannot be made since the diagonal components of P_{ij} do not depend on ϕ. However, the polarized neutron data do allow both the Mn moments and the angle ψ to be determined with good precision. A least squares fit to the structure with magnetic space group $P6'_3$ gave $\mu = 3.14(3)\ \mu_B$ and $\psi = 10.9(8)°$ with a goodness of fit $\chi^2 = 3.4$ compared with $\chi^2 = 11$ for the structures in which the mirror planes were retained.

5.3. Magnetic structures of $HoMnO_3$

In contrast to what was found for $YMnO_3$ in $HoMnO_3$, there are no very significant differences between the three diagonal elements of the polarization matrices of $h0.l$ reflections with odd l. Some depolarization is observed, but can be attributed to multiple nuclear scattering in

the weaker reflections. The P_{zz} component is positive at 50 K and negative at 20 and 1.8 K, which is consistent with the reported transition from $P6'_3c'm$ to $P6'_3cm'$ in which the Mn moments rotate by 90°. The symmetry $P6'_3c'm$ is not compatible with ordered moments on the Ho1 atoms; it constrains any ordered moments on Ho2 to be parallel to [00.1] and arranged in anti-ferromagnetic layers, anti-ferromagnetically coupled. In the space group $P6'_3cm'$, Ho moments on both sites can be ordered parallel to [00.1] in ferromagnetic layers, anti-ferromagnetically coupled. Ordering of the Ho moments will add components parallel to [00.1] to the magnetic structure factor, but only to the odd-l reflections because of anti-ferromagnetic coupling between moments separated by $\boldsymbol{c}/2$. At 50 K such Ho ordering would have been apparent in the polarimetric data by rotation of the scattered polarization towards y, but below the spin rotation transition, it only changes the scattered intensity and not its polarization since the interaction vector due to Mn ordering is already parallel to y. The polarimetric data for the even-l reflections were used in least squares determinations of the Mn moments at 50, 20 and 1.8 K using nuclear structure factors calculated with the parameters determined from the integrated intensity measurements. The values obtained were 2.46(5), 3.04(6) and 3.03(6) μ_B at 50, 20 and 1.8 K, which are slightly smaller than those obtained from the integrated intensity measurements table 5. The latter may have been over corrected for extinction if the magnetic (180°) domains are smaller than the ferroelectric ones [21]. Confirmation of the assignment of the α (a) structure $P6'_3cm'$ (figure 1) to $HoMnO_3$ at low temperatures can be obtained from the polarization matrices measured for $hh.l$ reflections. If x_{Mn} is exactly 1/3, the Mn contribution to the magnetic structure factor for $hh.l$ reflections is zero; on the other hand both Ho sites should contribute to these structure factors when l is odd. The l odd reflections in table 7 do indeed show significant depolarization in the P_{xx} component, indicating mixed magnetic and nuclear scattering. This is particularly apparent when the reflection intensity is small so that the magnetic part constitutes a significant fraction. $P_{xx} \approx P_{zz} < P_{yy}$ which shows that the magnetic interaction vectors are parallel to polarization y in agreement with the [00.1] orientation of the Ho moments. However, the magnetic scattering in the $hh.l$ reflections is very weak because the two Ho sites scatter with opposite phase and the polarization data are not sufficiently precise or numerous to allow a better determination of the Ho moments than that obtained from the integrated intensity measurements.

6. Discussion

It can be seen from table 5 that in both $YMnO_3$ and $HoMnO_3$ the manganese x parameter, x_{Mn}, is not significantly different from 1/3. In $HoMnO_3$ it does not change by more than 0.0008 on cooling from 50–2 K; no evidence was found for the sudden drop in x_{Mn} from 0.338 to 0.324 reported by [2] between 10 and 5 K. In fact there appears to be no significant change at all in the crystal structure between 2 and 50 K.

The variation with temperature of the Mn and Ho moments in $HoMnO_3$ is shown in figure 2(a). The values were obtained from least squares refinements assuming that there was no change in the magnetic structure between 20 and 2 K. The moments can be seen to increase smoothly with decreasing temperature. The data give no evidence for the change in symmetry at 5 K proposed by [2] and [20], which would imply a fundamental reorganization of the Ho ordering. The magnetic space group $P6_3cm$ does not allow ordered moments at the Ho1 sites, and requires anti-ferromagnetic alignment of the Ho2 moments within the hexagonal layers. Figure 2(b) shows the integrated intensities of pairs of {10.0} and {10.1} reflections measured at closely spaced temperature intervals between 2 and 15 K. The intensities measured for the {10.0} reflections are nearly constant in this temperature range. In our zero-field experiment we do not see the abrupt increase in the intensity of the {10.0} reflections below about 5 K

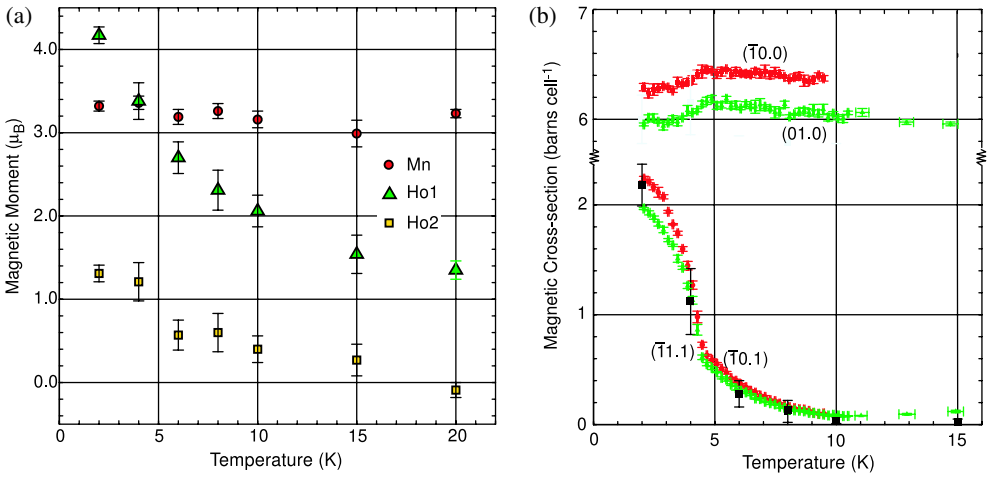

Figure 2. (a) Values of the ordered moments obtained from least squares fits to the integrated intensities measured for $HoMnO_3$ between 2 and 20 K. (b) The integrated intensities of {10.0} and {10.1} reflections of $HoMnO_3$ measured between 2 and 15 K; the black squares show the intensity of the {10.1} reflections calculated using the moments obtained from the least squares fits. Note the break in the intensity axis between 2 and 6 barn cell^{-1}. For both (a) and (b) at all temperatures the calculations are based on the model with magnetic group $P6'_3cm'$.

(This figure is in colour only in the electronic version)

reported by [20]. Such an increase is difficult to explain since in the present model, and in its homometric partner, proposed by [2] for the structure below 5 K, the Ho moments make no contribution to the {10.0} reflections. In both models the {10.0} reflection intensity depends only on the Mn moments, which are expected to be essentially saturated in this temperature range. The temperature variation of the {10.1} reflections follows closely that predicted for the $P6'_3cm'$ model with Ho moments obtained from the least squares fits. Between 20 and 12 K the intensity decreases because the Ho and Mn contributions are out of phase. Below about 12 K, as the Ho continues to order, the Ho scattering outweighs that from Mn and the intensity rises steeply.

It may be worth pointing out that for this symmetry there is a difference in the magnetic interaction vectors, and presumably also in the free energy, between the model derived here and one in which all the Mn moments are reversed but the Ho moments are not. This may be difficult to understand because the Mn and Ho moments are orthogonal. It arises because there is a chiral vector parallel to [00.1] associated with each triangle of Mn moments. The Ho moments interact with this vector and, since the oppositely oriented Ho moments are at unequal distances from these triangles, there is a resultant interaction which changes sign when the Mn moments reverse and the Ho moments do not. It is the correlation between the sign of this interaction and the direction of the structural polarization which distinguishes the configurations. The intensity and polarimetric data measured in this experiment show that the energetically favourable configuration is that in which the moments on all the Ho1 and Mn1 atoms point either towards or away from their nearest O3 neighbour, as shown in figure 3.

In $YMnO_3$ it is clear from the polarimetric data that the magnetic structure has lower symmetry than $6mm$. The neutron results are equally compatible with the magnetic groups $P6'_3$ and $P6_3$, but the absence of a magneto-electric effect and the SHG results both favour $6'_3$. The SHG spectra [12] suggested $P6'_3cm'$; however, the angle ψ by which the moment

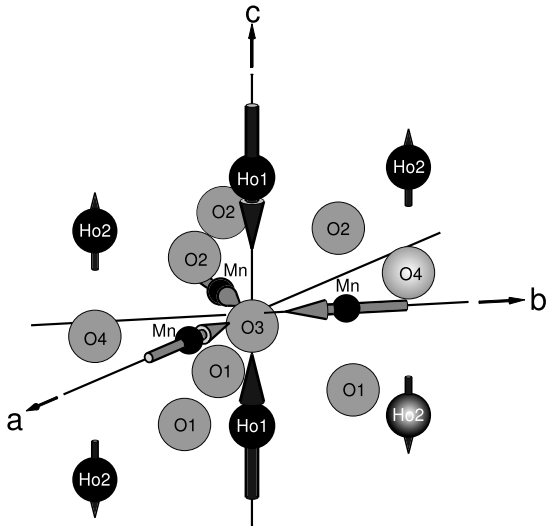

Figure 3. Schematic drawing of a fragment of the magnetic structure of $HoMnO_3$ at 2 K, showing the orientation of the moments around the origin of the unit cell.

deviates from the axial directions is only 11°, which might not have been resolved in the SHG experiments.

In conclusion, we have shown that neutron polarimetry combined with single crystal neutron diffraction up to high $\sin\theta/\lambda$ can in general allow distinction to be made between magnetic structure models which give nearly identical diffraction intensities. The present study shows that caution should be exercised when using the results of SHG experiments. However, combining the SHG and neutron results has enabled the zero-field magnetic structures of both $YMnO_3$ and $HoMnO_3$ to be determined with some certainty.

Acknowledgments

We are grateful to Dr T Lonkai for critical discussion and his help during the experiment and would like to thank Dr W Kohn for supplying us with the $YMnO_3$ and $HoMnO_3$ crystals.

References

[1] Huang Z J, Cao Y, Sun Y Y, Xue Y Y and Chu C W 1997 *Phys. Rev.* B **56** 2623
[2] Lottermoser T, Lonkai T, Amann U, Hohlwein D, Ihringer J and Fiebig M 2004 *Nature* **30** 541
[3] Katsufuji T, Mori S, Masaki M, Moritomo Y, Yamamoto N and Takagi H 2001 *Phys. Rev.* B **64** 04419
[4] Fiebig M, Lottermoser T, Frölich D, Goltsev A V and Pisarev R V 2002 *Nature* **419** 818
[5] Sato T J *et al* 2003 *Phys. Rev.* B **68** 14432
[6] Park J *et al* 2003 *Phys. Rev.* B **68** 104426
[7] Bertaut E F and Mercier M 1963 *Phys. Lett.* **5** 27
[8] Bertaut E, Pauthenet R and Mercier M 1967 *Phys. Lett.* **18** 13
[9] Munõz A *et al* 2000 *Phys. Rev.* B **62** 9498
[10] Lonkai T, Hohlwein D, Ihringer J and Prandl W 2002 *Appl. Phys.* A **74** S843
[11] Lonkai T *et al* 2003 *J. Appl. Phys.* **93** 8191
[12] Fiebig M *et al* 2000 *Phys. Rev. Lett.* **84** 5620
Frölich D, Leute St, Pavlov V V and Pisarev R V 1998 *Phys. Rev. Lett.* **81** 3239
[13] Yakel H L, Koehler W C, Bertaut E F and Forrat E F 1963 *Acta Crystallogr.* **16** 957

[14] Koehler W C, Yakel H L, Wollan E O and Cable J W 1964 *Phys. Lett.* **9** 3
[15] Bacon G E 1975 *Neutron Diffraction* (Oxford: Oxford University Press) pp 488–95
[16] Brown P J 2001 *Physica* B **297** 198
[17] Tasset F *et al* 1999 *Physica* B **267/268** 69
[18] Lelièvre-Berna E 2002 *Proc. SPIE* **4785** 112
[19] Becker P J and Coppens P 1974 *Acta Crystallogr.* A **30** 129
[20] Vajk O P, Kenzelmann M, Lynn J W, Kim B and Cheong S-W 2005 *Phys. Rev. Lett.* **94** 87601
[21] Brown P J, Nunez V, Tasset F and Forsyth J B 1992 *Acta Crystallogr.* A **48** 236